Anisotropic fluctuations and quasiparticle excitations in $FeSe_{0.5}Te_{0.5}$

A. Serafin,[1] A. I. Coldea,[1,*] A. Y. Ganin,[2] M. J. Rosseinsky,[2] K. Prassides,[3] D. Vignolles,[4] and A. Carrington[1]
[1]*H.H. Wills Physics Laboratory, University of Bristol, Tyndall Avenue, Bristol BS8 1TL, United Kingdom*
[2]*Department of Chemistry, University of Liverpool, Liverpool L69 7ZD, United Kingdom*
[3]*Department of Chemistry, Durham University, South Road, Durham DH1 3LE, United Kingdom*
[4]*Laboratoire National des Champs Magnétiques Intenses, CNRS, 143 Avenue de Rangueil, 31400 Toulouse, France*
(Received 22 July 2010; revised manuscript received 25 August 2010; published 20 September 2010)

We present data for the temperature dependence of the magnetic penetration depth $\lambda(T)$, heat capacity $C(T)$, resistivity $\rho(T)$, and magnetic torque τ for highly homogeneous single-crystal samples of $Fe_{1.0}Se_{0.44(4)}Te_{0.56(4)}$. $\lambda(T)$ was measured down to 200 mK in zero field. We find $\lambda(T)$ follows a power law $\Delta\lambda \sim T^n$ with $n=2.2\pm0.1$. This is similar to some 122 iron arsenides and likely results from a sign-changing pairing state combined with strong scattering. Magnetic fields of up to $B=55$ or 14 T were used for the $\tau(B)$ and $C(T)/\rho(T)$ measurements, respectively. The specific heat, resistivity, and torque measurements were used to map out the (H,T) phase diagram in this material. All three measurements were conducted on exactly the same single-crystal sample so that the different information revealed by these probes is clearly distinguished. Heat-capacity data strongly resemble those found for the high-T_c cuprates, where strong fluctuation effects wipe out the phase transition at H_{c2}. Unusually, here we find the fluctuation effects appear to be strongly anisotropic.

DOI: 10.1103/PhysRevB.82.104514 PACS number(s): 74.70.Xa

I. INTRODUCTION

The superconducting iron-chalcogenide compounds $Fe_{1+y}Se_{1-x}Te_x$ have attracted much interest because of their many similarities to the high-T_c iron pnictides. The transition temperature can be varied between 8 and 14 K by changing the chalcogenide ratio x and reaches a maximum at around $x=0.5$ ($y\simeq0$).[1] These materials share the structural motif of square planar sheets of tetrahedrally coordinated Fe with the iron-pnictide 1111 and 122 compounds [e.g., $SmFeAsO_{1-x}F_x$ with $T_c=55$ K (Ref. 2) and $Ba_{1-x}K_xFe_2As_2$ with T_c up to 38 K (Ref. 3)]. The iron-chalcogenide compounds are structurally simpler than their iron-pnictide counterparts because there are no guest ions or interleaved layers separating the iron-chalcogenide layers. Like the iron pnictides, the Fermi surface of these compounds is composed of quasi-two-dimensional electron and hole pockets located at the Brillouin-zone corner (M point) and center (Γ) point, respectively.[4,5] It is likely therefore, that if the unusual Fermi-surface topology is the ultimate origin of the pairing interaction then we might expect the mechanism to be similar in these materials.

In this paper, we report measurements of two aspects of the physics of the highest T_c member ($x\simeq0.5$) of the $Fe_{1+y}Se_{1-x}Te_x$ series. First, we show data for the magnetic penetration depth $\lambda(T)$ in the superconducting state. These measurements give information about the pairing interactions which drive the superconductivity. Second, we show measurements of the heat-capacity, magnetic torque, and electrical resistivity of exactly the same single-crystal sample. These measurements are used to derive the temperature-field phase diagram of this material. By performing the measurements on the same sample, the different points on the phase diagram measured by these probes are made clear. These measurements show several unusual features, most notably, that unlike some other iron-based superconductors the thermodynamics of the superconducting transition are dominated by strong thermal fluctuation effects (such as the high-T_c cuprate superconductors). However, unlike other superconductors these fluctuations effects appear to be strongly anisotropic.

A powerful way to understand what drives the superconducting pairing interaction is to determine the $\boldsymbol{k}$-dependent structure of the superconducting energy gap Δ. If the pairing interaction $v_{\boldsymbol{kk}'}$ is repulsive in some (or all) directions in $\boldsymbol{k}$ space, as expected for most spin-fluctuation-driven pairing models, then it is likely that Δ will change sign at some point on the Fermi surface.[6] In materials where there is a single sheet of Fermi surface, this inevitably results in gap nodes, i.e., points on the Fermi surface where the energy gap is zero. However, in the iron-based materials the existence of disconnected electron and hole sheet of Fermi surface means that the sign change can be accommodated between two different Fermi-surface sheets so that there are no nodes on either.[7–10] Such as state which is known as the $s_{\pm}$ state appears to be preferred if the scattering is dominated by wave vectors close to $\boldsymbol{q}=(\pi,\pi)$. However if there is strong intraband scattering (with low $\boldsymbol{q}$) then a state with nodes on the hole and/or electron sheets may be favored.[11–13]

Experiments to determine the gap anisotropy in the iron-based compounds have been conducted on many different iron-based superconductors. A variety of different behaviors have been found which might be explained by a combination of varying levels of sample disorder and in some cases intrinsic differences in the pairing state. The first single-crystal measurements of the temperature-dependent penetration depth were reported for the 1111 family compounds $PrFeAsO_{1-x}$ ($T_c=35$ K) (Ref. 14) and $SmFeAsO_{1-x}F_x$ ($T_c=44$ K).[15] These measurements showed that for $T\lesssim0.2T_c$ $\lambda(T)$ had a very weak temperature dependence compatible with a fully gapped state. Fitting the full temperature dependence (up to T_c) of the superfluid density required a model with two isotropic (s-wave) gaps. Experiments on the Co-doped Ba122 compound, $Ba(Fe_{1-x}Co_x)_2As_2$ ($T_c=13-24$ K)

(Ref. 16) showed a robust power-law behavior of $\lambda(T) \propto T^n$ with exponent n in the range 2–2.5, which might have been explained by a nodal gap in the presence of strong disorder.[17] However, measurements[18] of thermal conductivity κ did not find a substantial value of κ/T in the $T=0$ limit as would be expected for a sign changing line node in the gap and theoretical calculations[19–22] suggested that the observed power law in $\lambda(T)$ could result from the influence of strong-pair breaking interband scattering on the intrinsically fully gapped $s_{\pm}$ state. Strong disorder may be unavoidable in these systems because of the doping of Co into the conducting FeAs plane. On the other hand, LaFePO is a stoichiometric system in which the quasiparticle mean-free paths are long enough for quantum oscillations to be observable at relatively low field.[23] In LaFePO, $\lambda(T)$ was found to vary close to linearly with temperature which is strongly indicative of line nodes in the clean limit.[24] Although LaFePO has a relatively low T_c of 6 K, similar behavior was also seen in $BaFe_2(As_{0.66}P_{0.33})_2$ with $T_c=30$ K.[25] In both cases, a large value of $\kappa/T|_{T\to 0}$ was found,[25,26] which further supports the conclusion that at least some of the Fermi-surface sheets have line nodes in these compounds. So the evidence suggests that the pairing state is not the same in all iron-based superconductors. It has been suggested that the different behaviors are driven by the orbital character of the hole sheets which are in turn determined by the height of the pnictogen atom.[12] Kogan[21] has recently shown that if strong pair breaking is responsible for the T^2 power-law behavior of $\lambda(T)$ in the iron pnictides then the coefficient of this T^2 term should be related to the height of the mean-field part of the specific-heat jump at T_c and the slope of the upper critical field dH_{c2}/dT. We use our data for $FeSe_{0.5}Te_{0.5}$ to make a quantitative test of this theory.

II. EXPERIMENTAL DETAILS

The single crystals used in this work were grown from the elements using iodine as the vapor transport medium at 680 °C targeting the nominal composition $Fe_{1.0}Se_{0.5}Te_{0.5}$. The details of the synthesis are reported elsewhere.[27] The crystal structure of the exact sample measured here (sample 1) was determined by single-crystal x-ray diffraction (XRD). No extra iron was observed between the Fe(Se/Te) slabs so the mean formula was identified as $Fe_{1.0}Se_{0.44(4)}Te_{0.56(4)}$. This was additionally confirmed by energy-dispersive x-ray (EDX) analysis.

The magnetic penetration depth as a function of temperature has been measured in three different single crystals [typical dimensions (sample 1) $300\times400\times4$ μm^3 with the smallest dimension along the c axis], using a radio-frequency tunnel diode oscillator.[28] The sample was mounted with vacuum grease on a cold-finger sapphire rod which was inserted into a copper wound solenoid forming the inductor of a resonant LC circuit with frequency close to 12 MHz. The rf field was orientated along the c axis of the crystal, thus only in-plane screening currents were excited. The experiment was shielded from external fields using a mu-metal can and the probe field was $\lesssim 10^{-6}$ T thus minimizing any contributions from mobile vortices. Two different experimental setups were used. One is mounted in a pumped ^{4}He cryostat with base temperature $\sim$1.4 K and the second in a dilution refrigerator where the sample may be cooled below 100 mK (here the resonant frequency is $\sim$14 MHz).[29] The calibration factor relating the measured frequency shifts with temperature to $\Delta\lambda(T)$ was determined from the geometry of the sample, and the total perturbation to the resonant frequency due to the sample, found by withdrawing the sample from the coil at low temperature. The procedure is described in more detail in Ref. 30.

The heat capacity of sample 1 from the penetration depth study (mass $\simeq 3$ μg) was measured using a temperature modulation technique. We use light as a heat source to minimize addenda and make the heating uniform over the sample surface, however this does mean that the absolute power (and hence heat capacity) are difficult to estimate accurately so our data for C are left in arbitrary units. Also the addenda are difficult to determine as the length of thermocouple wire which contributes depends on the presence or absence of the sample. Despite these limitations, the method is able to measure very small samples of order 1 μg over a wide temperature range with very high resolution. These smaller samples are usually much more homogeneous with sharper superconducting transitions than larger samples. The sharp transition was critical for the accurate characterization of the fluctuation effects as will be explained in more detail below. As our present study is focused on studying the evolution of the nature of the superconducting phase transition with magnetic field the lack of absolute scale for C is not a serious limitation.

The sample was glued with a small amount of VGE-7031 varnish to a flattened thermocouple made from 12 μm diameter Chromel and Constantan wires (type E).[31] The sample and thermocouple couple were then attached to a temperature controller stage in a vacuum enclosure which sits in the ^{4}He bath of a 14 T superconducting solenoid. The sample was heated using a modulated light source which was generated by an infrared light-emitting diode (LED) at room temperature and directed onto the sample using a plastic optic fiber. The size of the temperature oscillations T_{ac} is inversely related to the heat capacity C of the samples, $T_{ac}=P/\omega C\times f(\omega)$, where P is the power of the sinusoidal heat source (light) at frequency ω.[3] The function $f(\omega)$ depends on the time constants of the setup and the operating frequency (typically 6–20 Hz) is chosen to be the frequency where ωT_{ac} has the minimum frequency dependence in the temperature range of interest.[32] This ensures that $f(\omega)$ remains relatively constant as the experimental time constants change as a function of temperature and therefore $C\propto T_{ac}^{-1}$. The temperature of the LED is stabilized to minimize drift. The temperature of the stage was monitored using a Cernox 1050 thermometer, the magnetoresistance of which was corrected for using the data of Ref. 33 (although this is negligible in the temperature range of interest for the present study). In zero magnetic field, the thermopower of the thermocouple was taken from the standard table for type-E thermocouples.[34] The field dependence of the thermocouple sensitivity was estimated by measuring the field dependence of the temperature oscillations when a high-purity Ag sample (coated with a thin layer of black ink to maximize the light

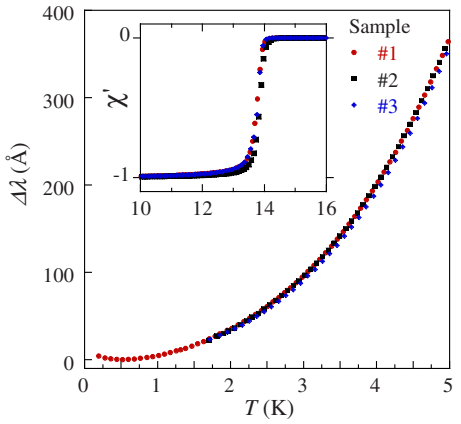

FIG. 1. (Color online) Temperature-dependent in-plane penetration depth for three samples of $FeSe_{0.5}Te_{0.5}$. For sample 1, $\Delta\lambda$ is relative to the minimum value measured (at $T=0.52$ K) whereas for samples 2 and 3, the data have been shifted to coincide with sample 1 at $T=1.7$ K which was the lowest temperature to which these samples were measured. The inset shows the rf susceptibility (normalized to −1 at $T\simeq 0$ and 0 in the normal state) close to T_c. The three samples show sharp superconducting transitions ($\Delta T_c \sim 0.5$ K).

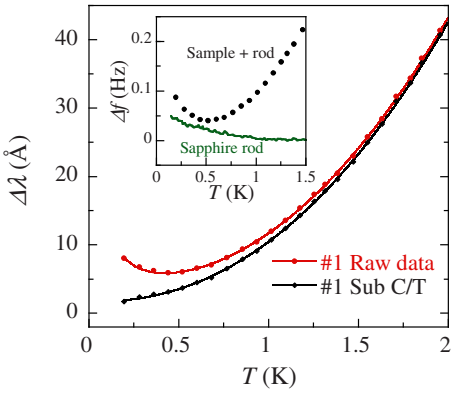

FIG. 2. (Color online) Low-temperature behavior of the penetration depth in sample 1 from Fig. 1. The main figure shows the temperature dependence of the sample with the background from the sapphire rod subtracted (red circles) and also with the fitted paramagnetic term subtracted (black diamonds). The lines are fits to a power law (black line) and power law plus Curie term (red line) as described in the text. The inset shows the measured oscillator frequency shifts for the sample plus sapphire rod and also the sapphire rod alone.

absorption) replaces the sample on the same thermocouple. At $T=15$ K, the sensitivity changes by ~4% between 0 and 14 T whereas at $T=24$ K, the change is ~2%.

Electrical resistivity was measured on a small piece cut from sample 1 (dimensions $310\times75\times4$ μm^3) using the standard four-probe method with an ac current excitation of 100 μA. Contacts were made using pressed Au, which resulted in contact resistances of a few ohm.

Magnetic torque was measured using a piezoresistive cantilever technique[35] on another small piece cut from sample 1 (dimensions $70\times100\times4$ μm^3). Here the resistance of an atomic force microscopy cantilever is measured using Wheatstone bridge arrangement with an ac excitation current of 10 μA at 72 Hz. The sample was attached to the cantilever with vacuum grease and mounted in vacuum on a rotating platform in the 14 T magnet. Checks were made at different current levels to ensure that there is no significant self-heating of cantilever and sample in the temperature range of interest. Samples from the same batch were also measured using the same technique but with pulsed fields up to 55 T in Toulouse. Here the sample/cantilever is surrounded by ^{4}He exchange gas or liquid.

III. RESULTS

A. Magnetic penetration depth

Data for the temperature dependence of λ for three of our samples of $FeSe_{0.5}Te_{0.5}$ are shown in Fig. 1. All three samples show a very sharp superconducting transition at $T_c=13.8$ K (midpoint) ($\Delta T\sim0.5$ K), and very similar low-temperature behavior (only sample 1 was measured below 1.7 K). The absolute temperature dependence of the $\Delta\lambda(T)$ is quite reproducible (to within 10%) indicating that the calibration factor has been accurately determined and that there are no complications from rough edges which can lead to an overestimation of the absolute scale of $\Delta\lambda(T)$.[36]

The low-temperature behavior is shown more clearly in Fig. 2. Below $T\simeq0.5$ K there is a small upturn in $\Delta\lambda(T)$. Note that the contribution from the sapphire rod on which the sample is mounted is smaller and has a significantly weaker temperature dependence (see inset of Fig. 2). The contribution from the rod has been subtracted from the data in the main panel. The likely origin of this upturn is a Curie-type paramagnetism of the normal state. In general, the measured penetration depth λ_m is related to the London depth (λ_L) by $\lambda_m(T)=\lambda_L(T)\sqrt{1+\chi_N(T)}$, where $\chi_N(T)$ is the normal-state susceptibility.[37] Assuming a simple Curie law form for $\chi_N(T)$ then for $\chi_N(T)\ll1$ the additional contribution to the measured penetration depth is given by

$$\Delta\lambda_{NP}=\frac{n_i\lambda_L(0)\mu_0\mu_e^2}{6k_BV_{\rm cell}T}, \tag{1}$$

where n_i is the number of magnetic ions per unit cell, $V_{\rm cell}$ is the unit-cell volume (=86.2 Å^3), and μ_e is the effective magnetic moment of the paramagnetic ion. In Fig. 2, we show a fit of the low-temperature $\lambda(T)$ data to a power-law dependence plus the $\Delta\lambda_{NP}$ contribution,

$$\Delta\lambda(T)=AT^n+\frac{\mathcal{C}}{T}+\lambda_{\rm offset}. \tag{2}$$

This equation fits the data very well, with $n=2.2\pm0.1$, $\mathcal{C}=1.24$ Å/K. This value of $\mathcal{C}$ corresponds to an average moment of $0.16\mu_B$ per unit cell [assuming $\lambda_L(0)=5000$ Å].[38] A fit using a Curie-Weiss form $\chi_N=\mathcal{C}/(T+T_\theta)$ gives a slightly better fit (not shown) however as the fitted value of $T_\theta=0.16$ K is below our minimum temperature this should be viewed with some caution (for this fit $\mathcal{C}=3.0$ Å/K and the exponent n was unchanged). This small moment could come from the bulk Fe atoms or possibly from a small amount of

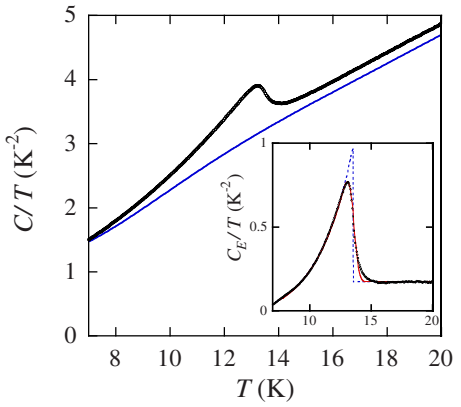

FIG. 3. (Color online) Zero-field total heat-capacity data. Here we have set the constant of proportionality between C and T_{ac}^{-1} to unity so the size of the applied temperature oscillations can be read off the axis. The solid blue curve is the estimated nonelectronic background coming from the sample phonon heat capacity and also the addenda. The inset shows the electronic part of C with the background subtracted together with the alpha-model fit (blue curve). The green curve shows the same fit convoluted with a Gaussian T_c distribution, $T_c^0=13.60$ K and $\sigma_{T_c}=0.32$ K.

free Fe impurities (although we note that none were detected in this sample by the XRD or EDX measurements).

The observed power law is close to 2, and as discussed above could either indicate a nodal state in the presence of disorder or instead could result from strong interband scattering between two intrinsically fully gapped Fermi-surface sheets with sign-changing gap between the sheets ($s_\pm$ state). Thermal-conductivity measurements[39] on the related compound $FeSe_x$ ($T_c=8.8$ K) show that $\kappa/T|_{T\to 0}$ is less than 4% of its normal-state value suggesting the absence of sign-changing nodes at this composition. As far as we are aware there have been no $\kappa(T)$ data published for $FeSe_{0.5}Te_{0.5}$, so for this composition the existence or not of nodes is still an open question.

Previously, penetration depth measurements have been performed by the muon-spin rotation/relaxation technique as well as a tunnel diode oscillator (TDO) technique similar to that used here. The μSR results of Bendele *et al.*[40] for $x=0.5$ ($T_c=14$ K) were interpreted using a two-gap s-wave model, however the data show no evidence for saturation of $\lambda^{-2}(T)$ at low T due to the lack of data below $T=1.5$ K ($T/T_c\simeq 0.1$). The μSR data of Biswas *et al.*[38] for a similar composition did show saturation at low temperature and were also fitted by a two-gap s-wave model. However, the fact that μSR measurements are conducted in the mixed state means that these results are not definitive.[38,41] The TDO measurements of Kim *et al.*[42] were reported on samples with $x=0.37$ ($T_c\sim 14$ K). These data show a power law $\lambda\sim T^n$ down to the lowest temperatures ($T\simeq 0.5$ K) with $n=2.1$ which is consistent with our findings for $FeSe_{0.5}Te_{0.5}$.

B. Heat capacity

The heat capacity of sample 1 (from the penetration depth study) is shown in Fig. 3. In order to make the evolution of the sample's electronic heat capacity with field clearer, we have estimated the background (which includes the samples phonon heat capacity and the addenda) in the following way. We fitted the zero-field data over the full temperature range to a polynomial (fifth order) to model the nonelectronic terms plus the electronic heat capacity calculated using a single-gap alpha model. In the alpha model,[43] strong-coupling effects are modeled by multiplying the weak-coupling s-wave BCS temperature-dependent energy gap $\Delta(T)$ by a constant α, and then the heat capacity is calculated in the standard way. The model works because the temperature-dependent strong-coupling corrections to $\Delta(T)$ are less important than the zero-temperature value of $\Delta(T)$ for the behavior of C. For the purposes of the current study, we can simply regard this as an entropy conserving construction for estimating the field-independent background. Note that the assumption of s- or d-wave behavior for $\Delta(T)$ makes insignificant differences in this range of temperature ($T/T_c \gtrsim 0.5$) besides changing α.[44] The excellent fit of this model to the data is shown in Fig. 3, gives $\Delta_0/T_c=3.2$, which might indicate strong coupling (for elemental Pb $\Delta_0/T_c=2.25$).

In the subtracted data, some broadening of the superconducting transition is evident, which comes from both sample inhomogeneity (a distribution of T_c values) and also strong thermal fluctuation effects (see later). In order to quantify the sample inhomogeneity effect in Fig. 3, we show a fit to the data with the alpha model convoluted with a Gaussian T_c distribution, i.e., $C(T)=\int_{-\infty}^{\infty}C(T,T_c)P(T_c)dT_c$ with the probability distribution function $P(T_c)=\exp[-(T_c-T_c^0)^2/(2\sigma_{T_c}^2)]/\sqrt{2\pi\sigma_{T_c}^2}$ and $C(T,T_c)$ fixed by the above non-convoluted alpha-model fit. As show in the inset of Fig. 3, this fits the data well with $T_c^0=13.60$ K and $\sigma_{T_c}=0.32$ K. As fluctuation effect have not been included here (for simplicity), this gives an upper limit on the sample inhomogeneity as $\sigma_{T_c}/T_c^0\simeq 2\%$. Note that this distribution of T_c in the sample has no intrinsic connection to the scattering possible responsible for the T^2 behavior of the penetration depth.

The field dependence of the electronic heat capacity (i.e., raw data with the polynomial background in Fig. 3 subtracted) for the same sample measured in both field directions ($B\|c$ and $B\|ab$) is shown in Fig. 4. There is a clear striking difference in the behaviors in the two field directions. For $B\|ab$, the behavior is close to that found for conventional type-II superconductors. The superconducting anomaly shifts down in temperature with the peak slightly decreasing in height (25% in 14 T), and the transition temperature width remains almost constant. However, in the $B\|c$ direction the anomaly is very strongly broadened by the field with the onset temperature remaining roughly field independent. The anomaly height is reduced by ~40% in 14 T. This qualitative difference is clearly illustrated in Fig. 5 where we compare directly the $B\|c$ and the 14 T $B\|ab$ data. The reduction in anomaly height for 14 T $B\|ab$ data is comparable to that found for 4 T $B\|c$, however, the broadening is not comparable at any field.

The behavior for $B\|c$ is similar to that found on high-T_c cuprate superconductors where the thermodynamics of the superconducting transition are dominated by strong (critical) thermal fluctuation effects.[45–49] Unlike conventional low-T_c superconductors where the jump in C at T_c is almost a per-

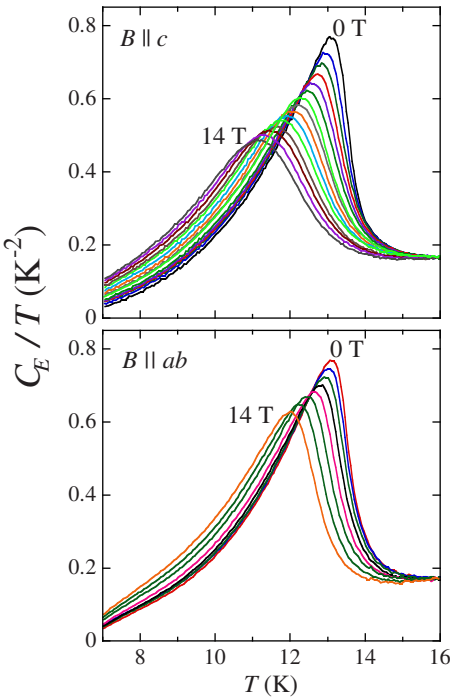

FIG. 4. (Color online) Field dependence of the electronic heat capacity (i.e., raw data with the polynomial background in Fig. 3 subtracted). In the upper panel, the field is perpendicular to the planes and increases in 1 T intervals from 0 to 14 T. In the lower panel, the field is parallel to the planes and increases in 2 T intervals from 0 to 14 T. Before subtraction of the background small (<1% of the total) corrections were applied to normalize all data to the same value at 16 K. This is necessary to correct for slight drift in the heating power. Field sweeps at this fixed temperature showed that $C(H)$ was constant (after correction for the thermocouple field dependence) within resolution.

fect example of a classic second-order phase transition, in $YBa_2Cu_3O_{6.9}$ (T_c=93 K) the anomaly resembles the λ anomaly found at the superfluid transition of ^{4}He which is well described by the three-dimensional (3D)-XY critical fluctuation model.[50] The broadening (with little or no reduction in onset temperature) and reduction in height of the anomaly is commonly observed in high-T_c cuprates.[45–49] There is some controversy regarding the best theoretical picture to describe this. Models based on finite-size scaling within the critical 3D-XY framework and fluctuation models based on the lowest Landau level (LLL) approximation have both been used.[46–48] In principle, it should be expected that the finite-size scaling should work best at low fields (compared to H_{c2} at T=0) and the LLL model at high fields.[46] The finite-size effects arise because the magnetic field introduces a new length scale $d_B=(\phi_0/\pi B)^{1/2}$, which limits the growth of the physical size of the fluctuations as T approaches T_c. When the transition is dominated by such strong fluctuation effects the true phase transition at H_{c2} is wiped out as the fluctuations in the order parameter are much larger than the mean value over a large range of (H,T) space close to the $H_{c2}(T)$ line.[51] The heat capacity still displays a broad hump at the "$H_{c2}(T)$" line but the resistivity for example does not become zero until lower temperature when the vortex lattice freezes and phase coherence is achieved. The strong fluctuation effects in high-T_c cuprates are driven by their short coherence lengths, low dimensionality, and high critical temperatures.[51] Compared to the cuprates, $FeSe_{0.5}Te_{0.5}$ is relatively isotropic and has a much lower T_c but does have a comparably short coherence length. The estimated irreversibility field at T=0 of $FeSe_{0.5}Te_{0.5}$ is similar to that found for underdoped $YBa_2Cu_3O_{6.5}$ (Ref. 52) or $YBa_2Cu_4O_8$ (Ref. 53).

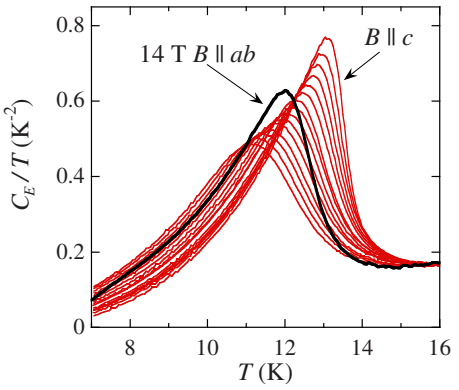

FIG. 5. (Color online) Comparison of the field-dependent heat capacity $C_E(H)$ for $B\|c$ with the 14 T data for $B\|ab$.

The field broadening of $C(T)$ for $B\|c$ is in contrast to the more conventional behavior observed in 122 compounds such as $BaFe_2(As_{0.66}P_{0.33})_2$ with T_c=30 K,[25] however evidence for strong fluctuation effects have been seen in the field-dependent heat capacity of the 1111 compound $NdFeAsO_{1-x}F_x$ (Ref. 54). An unusual aspect of the behavior of $FeSe_{0.5}Te_{0.5}$ is that the fluctuations effects appear to be strongly anisotropic. In $YBa_2Cu_3O_{6.9}$ although the $H_{c2}(T)$ and irreversibility field H_{irr} are anisotropic, the behaviors in the two directions are identical apart from a difference in the field scale (the heat capacity for 1 T$\|c$ is identical to 8 T$\|ab$).[47,49] Here the behaviors are qualitatively different in the two field directions. Fluctuations effects are minimal for $B\|ab$ but strong for $B\|c$. It would appear that in-plane field does not disrupt the phase coherence between the planes but for $B\|c$ the effective dimensionality is strongly reduced and fluctuations effects enhanced.

C. Resistivity

The temperature and field dependence of the resistivity of sample 1 is shown in Fig. 6. Although there is again more broadening of the transition for $B\|c$ compared to $B\|ab$ it is much less evident than that seen in the heat-capacity data. In the inset of Fig. 6, we show a direct comparison between the zero-field heat-capacity and resistivity data for the same sample. The midpoint of the resistive transition is ~0.75 K higher than the midpoint of the heat capacity. The peak in the heat capacity is a further 0.5 K lower and corresponds to the point where the resistivity is ~1% of its value just above T_c. This difference is understandable as a large reduction in the resistivity will be achieved when a sufficient amount of the sample to create a percolation path becomes superconducting. Often this amount will be much less than 50% but depends on the spatial distribution of T_c in the sample.

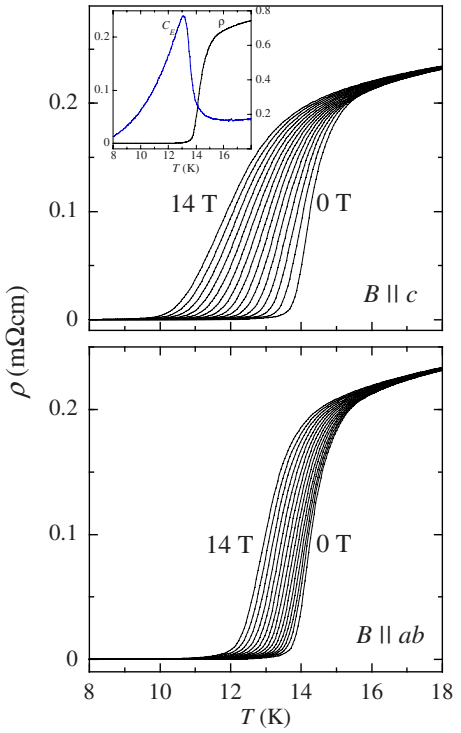

FIG. 6. (Color online) Resistivity versus temperature for sample 1 for fields between 0 and 14 T applied either parallel or perpendicular to c. The inset in the upper panel shows a direct comparison of the resistivity (left-hand scale) and heat capacity (right-hand scale) of the same sample (sample 1) in zero magnetic field.

D. Torque

Torque data in quasistatic fields up to 14 T for a small piece cut from the heat-capacity sample is shown in Fig. 7 at angles of approximately 5° from $B\|c$ and $B\|ab$. The angle offset is necessary because at the symmetry points, the torque is exactly zero. These small offset make negligible

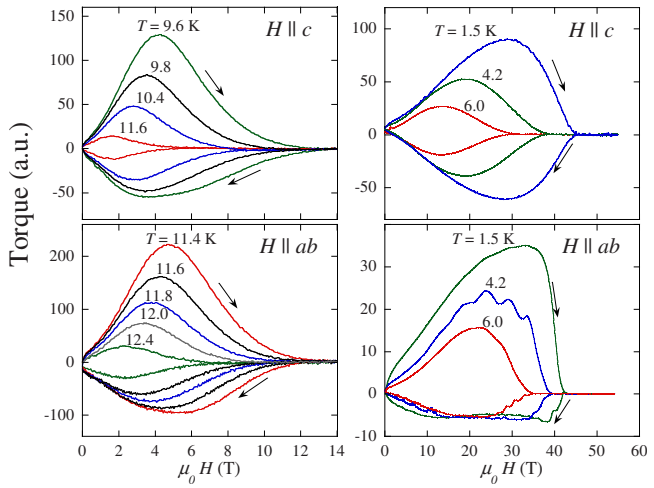

FIG. 7. (Color online) Torque hysteresis loops. The left two panels show data in quasi-dc field for a small piece cut from sample 1. The right two panels show data taken in pulsed field for a second sample. The field directions are actually ~5° from the symmetry directions indicated on the figure.

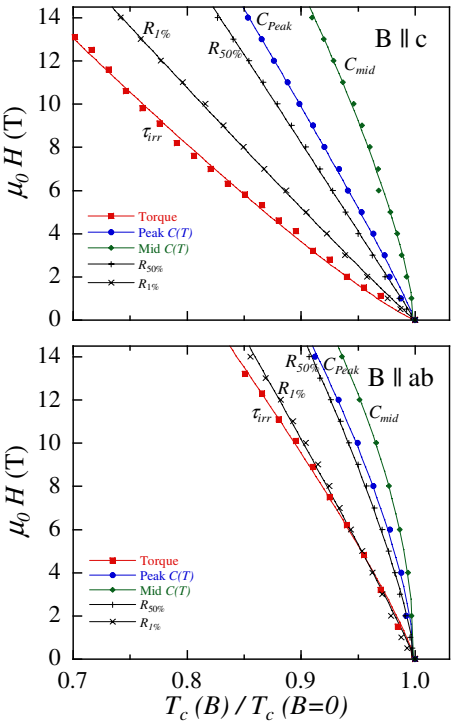

FIG. 8. (Color online) H-T phase diagram for $FeSe_{0.5}Te_{0.5}$ close to T_c derived from heat capacity, resistivity, and torque measurements. For the heat capacity, the temperature of the peak in $C(T)$ and the midpoint of the rise above the peak the transition are plotted. For the resistivity, $R_{50\%}$ and $R_{1\%}$ are the points at which the resistivity has fallen to 50% and 1% of extrapolated normal-state resistivity above T_c, respectively. For the torque the point where the hysteresis loop closes (within our resolution), i.e., the irreversibility field $\mu_0 H_{\rm irr}$ is plotted. The lines are fits to the power law $H = H_0(1-T/T_c)^n$, to guide the eyes.

difference to the derived irreversibility fields as the anisotropy is not strong. Data taken in pulsed fields for a different sample from the same batch is shown in Fig. 7. In both cases, the torque is strongly hysteretic indicating strong pinning. In the pulsed field $B\|c$ data oscillations are evident which likely arise from flux jumps. In all data, the torque loops close at within our resolution at an irreversibility field ($H_{\rm irr}$), and no further kinks at higher field (which might mark H_{c2}) are evident.

E. Phase diagram

A compilation of the data derived from the heat-capacity, resistivity, and torque measurements is plotted in Fig. 8 as a function of reduced temperature $T_c(B)/T_c(B=0)$. It is important to realize that in general these different experimental techniques will measure different points in the (H,T) phase diagram. For a superconductor without strong fluctuation effects there will be a step in the heat capacity at T_c which will be broadened by inhomogeneity and will shift down in temperature under applied field marking the $H_{c2}(T)$ line. The width of the broadened step in field will be related to the width in zero field and the slope of $H_{c2}(T)$. In this case the midpoint of the rise of $C(T)$ can be used to determine $H_{c2}(T)$.

However, in the present case, as the broadening of $C(T)$ in field cannot be explained by inhomogeneity alone there must also be strong thermal fluctuation effects as described above. In the case of phase transitions where fluctuation effects are strong, the peak in $C(T)$ is usually used to define the phase transition point, and so for the present case this likely gives the best estimate of $H_{c2}(T)$. At the point at which the magnetization becomes irreversible (the irreversibility line) the sample will acquire a finite critical current. Hence the irreversibility line as measured by our torque measurements marks the point where the critical current takes a finite value—the size of which depends on the resolution of the torque measurements. It should be expected that this irreversibility line is close to the point where the resistivity becomes zero as this is also where the critical current becomes equal to the resistivity measurement current. In the case that the irreversibility line and H_{c2} are not in close proximity it is difficult to know what point in the resistivity curve corresponds to $H_{c2}(T)$. For example, if the vortex viscosity is very low the resistivity in the mixed state will be close to the normal-state value and there will be almost no anomaly at $H_{c2}(T)$.[55,56]

In the present case, the peak in $C(T)$ coincides reasonably well with the point on the resistivity curve where the resistance has fallen to 50% of its extrapolated normal-state value ($R_{50\%}$). This is the case for *both* field directions (see Fig. 8). Hence is it reasonable to conclude that both of these two quantities are measuring the temperature dependence of H_{c2}. The 1% resistivity point ($R_{1\%}$) is better correlated with the torque irreversibility field as expected from the above discussion.

For $B\|c$, there is clearly a very marked difference between the irreversibility line derived from the torque measurements and the thermodynamic transition measured by specific heat. The average slope of the torque irreversibility field $dH_{\rm irr}^{\|c}/dT=-44$ T/K whereas for the peak in $C(T)$ it is -95 T/K and the midpoint -150 T/K. Hence estimates of H_{c2} from the irreversibility field for this field direction will serious underestimate the true values. Although the data are better fitted by a power law $H=(1-T/T_c)^n$ as indicated in the figure rather than a linear relation, the average slope still provides a useful rough comparison. The large separation between the irreversibility field and the peak in the specific heat which we expect to be close to the mean-field H_{c2} line is again reminiscent of the behavior found in the high-T_c cuprates and is strongly suggestive of strong fluctuation effects.[45–49] For $B\|ab$, the lines are much closer together. The corresponding values for the average slopes are -90 T/K, -160 T/K, and 200 T/K, respectively.

The anisotropy of H_{c2} derived from the specific-heat measurements is considerably less than that derived from the torque irreversibility field. Taking the peak in $C(T)$ as the most reliable measure of $H_{c2}(T)$, we see that for $B\|c$ it is almost linear with temperature whereas for $B\|ab$ there is some curvature close to $T_c(0)$. Above ~ 8 T where $H_{c2}^{\|ab}(T)$ is linear the anisotropy is small, $\frac{dH_{c2}^{\|ab}}{dT}/\frac{dH_{c2}^{\|c}}{dT}=1.2$.

Braithwaite *et al.*[57] have also reported a difference between critical fields determined by resistivity or heat-capacity measurements for $FeSe_{0.48}Te_{0.52}$. In their case, they found $R_{50\%}$ and the midpoint of the $C(T)$ curve approximately coincided for $H\|ab$ but not for $H\|c$. Their heat-capacity data showed almost no anisotropy. $C(T)$ data for $\mu_0 H=9$ T was almost independent of the field direction. It is likely that the differences in the $H\|ab$ data compared to ours are due to the much wider transition width of their sample. The zero-field $C(T)$ data in Ref. 57 are approximately three times wider than those here. The field broadened transition width of our data for $\mu_0 H=9$ T$\|c$ is comparable to the zero-field width in Ref. 57.

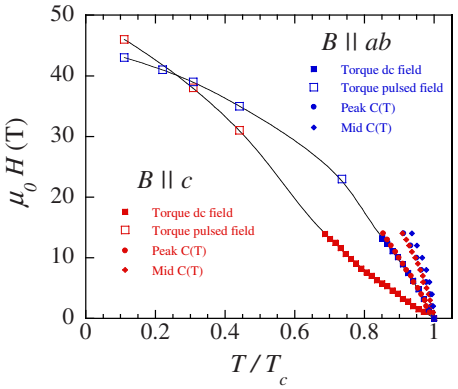

FIG. 9. (Color online) H-T phase diagram for $FeSe_{0.5}Te_{0.5}$ over the full range. The torque data mark the irreversibly line whereas the heat-capacity data $C(T)$ are two different estimates of the behavior of H_{c2}. The lines are guide to the eyes.

The phase diagram over a wide temperature-field range is shown in Fig. 9. As reported previously,[57,58] the irreversibility fields for the two field directions cross at low temperature with the anisotropy approaching unity. This and the general shape of these $H_{\rm irr}(T)$ curves, has been interpreted as evidence that H_{c2} is Pauli limited.[57,58] However, given the difference between $H_{\rm irr}$ and H_{c2} revealed by the lower field heat-capacity data, it is possible that this high-field behavior is also strongly influenced by thermal fluctuation effects and vortex pinning. High-field heat-capacity measurements will be necessary to determine whether the temperature dependence and anisotropy of H_{c2} follow that of $H_{\rm irr}$ at high field and low temperature.

IV. PAIR BREAKING

As mentioned in Sec. I, Kogan[21] has calculated that in anisotropic superconductors with strong pair breaking there should be a universal relationship between the coefficient of the T^2 term in the low-temperature penetration depth, the height of the mean-field part of the specific-heat jump $\Delta C_{\rm MF}$, and the slope of the H_{c2} near T_c. In SI units, the relation is

$$\Omega=\frac{\Delta C_{\rm MF}A^2T_c^4}{\left|\frac{dH_{c2}}{dT}\right|_{T_c}}=\frac{\phi_0}{4\pi}. \tag{3}$$

Note here that $\Delta C_{\rm MF}$ is units of J m^{-3} K^{-1} and ϕ_0 is the flux quantum. Fixing $n=2$ in Eq. (2), we get $A=10.3$ Å/K for the T^2 slope of the low-temperature $\lambda(T)$ data. As argued

above, the peak in $C(T,B)$ is likely to provide the best estimate of $H_{c2}(T)$ and from this we get $\mu_0 \frac{dH_{c2}}{dT} = 6.9$ T/K for $B \| c$ and T between $0.85T_c$ and $0.97T_c$. As our specific-heat data is not in absolute units, we estimate ΔC_{MF} from the data of Tsurkan *et al.*[59] for the specific heat of $FeSe_{0.5}Te_{0.5}$. This data is very similar to our own with regard to sharpness and value of T_c and slope of H_{c2}, and from this we estimate $\Delta C_{\mathrm{MF}} = 0.42$ J mol^{-1} K^{-1}. Taking the midpoint of the heat-capacity transition $T = 13.6$ K as T_c, we get from Eq. (3), $4\pi\Omega/\phi_0 = 0.65 \pm 0.15$ which is indeed close to unity as predicted by the Kogan theory (the uncertainty is dominated by that in T_c). Hence, it is likely that the T^2 behavior of the penetration depth does result from strong pair breaking. However, this does not rule out the possibility of intrinsic nodes if the material could be made sufficiently clean.

V. CONCLUSIONS

We have presented results for the temperature dependence of the magnetic penetration depth, heat capacity, and magnetic torque for highly homogeneous single-crystal samples of $Fe_{1.0}Se_{0.44(4)}Te_{0.56(4)}$. The penetration depth data display a power-law behavior $\Delta\lambda \propto T^n$ with $n = 2.2 \pm 0.1$, which is similar to some 122 iron arsenides. It is likely this results from the influence of strong pair breaking with a sign-changing pairing state which may or may not have intrinsic nodes.[19–22] Heat-capacity measurements have shown clear evidence for the presence of strong thermal fluctuations, at least for relatively low fields ($\mu_0 H \leq 14$ T). The behavior is reminiscent of the high-T_c cuprates, and like in these compounds we show that there is a sizable vortex liquid regime between the irreversibility line and the upper critical field. Unusually, the fluctuations influence the behavior with field along c much greater than for field along the planes.

ACKNOWLEDGMENTS

We thank John Bacsa for single-crystal XRD studies and Chris Ireland for the EDX measurements. We also thank Vladimir Kogan for drawing our attention to his pair-breaking theory. We acknowledge financial support from the Royal Society and EPSRC. Part of this work has been done with the financial support of EuroMagNET II under the EU Contract No. 228043.

*Present address: Clarendon Laboratory, Department of Physics, University of Oxford, Oxford OX1 3PU, United Kingdom.

[1] K. W. Yeh, T. W. Huang, Y. L. Huang, T. K. Chen, F. C. Hsu, P. M. Wu, Y. C. Lee, Y. Y. Chu, C. L. Chen, J. Y. Luo, D. C. Yan, and M. K. Wu, EPL **84**, 37002 (2008).
[2] Z. A. Ren, W. Lu, J. Yang, W. Yi, X. L. Shen, Z. C. Li, G. C. Che, X. L. Dong, L. L. Sun, F. Zhou, and Z. X. Zhao, Chin. Phys. Lett. **25**, 2215 (2008).
[3] M. Rotter, M. Tegel, and D. Johrendt, Phys. Rev. Lett. **101**, 107006 (2008).
[4] A. Subedi, L. J. Zhang, D. J. Singh, and M. H. Du, Phys. Rev. B **78**, 134514 (2008).
[5] A. Tamai, A. Y. Ganin, E. Rozbicki, J. Bacsa, W. Meevasana, P. D. C. King, M. Caffio, R. Schaub, S. Margadonna, K. Prassides, M. J. Rosseinsky, and F. Baumberger, Phys. Rev. Lett. **104**, 097002 (2010).
[6] D. J. Scalapino, Phys. Rep. **250**, 329 (1995).
[7] I. I. Mazin, D. J. Singh, M. D. Johannes, and M. H. Du, Phys. Rev. Lett. **101**, 057003 (2008).
[8] K. Kuroki, S. Onari, R. Arita, H. Usui, Y. Tanaka, H. Kontani, and H. Aoki, Phys. Rev. Lett. **101**, 087004 (2008).
[9] V. Cvetkovic and Z. Tesanovic, EPL **85**, 37002 (2009).
[10] A. V. Chubukov, D. V. Efremov, and I. Eremin, Phys. Rev. B **78**, 134512 (2008).
[11] S. Graser, T. A. Maier, P. J. Hirschfeld, and D. J. Scalapino, New J. Phys. **11**, 025016 (2009).
[12] K. Kuroki, H. Usui, S. Onari, R. Arita, and H. Aoki, Phys. Rev. B **79**, 224511 (2009).
[13] A. V. Chubukov, M. G. Vavilov, and A. B. Vorontsov, Phys. Rev. B **80**, 140515 (2009).
[14] K. Hashimoto, T. Shibauchi, T. Kato, K. Ikada, R. Okazaki, H. Shishido, M. Ishikado, H. Kito, A. Iyo, H. Eisaki, S. Shamoto, and Y. Matsuda, Phys. Rev. Lett. **102**, 017002 (2009).
[15] L. Malone, J. D. Fletcher, A. Serafin, A. Carrington, N. D. Zhigadlo, Z. Bukowski, S. Katrych, and J. Karpinski, Phys. Rev. B **79**, 140501(R) (2009).
[16] R. T. Gordon, C. Martin, H. Kim, N. Ni, M. A. Tanatar, J. Schmalian, I. I. Mazin, S. L. Bud'ko, P. C. Canfield, and R. Prozorov, Phys. Rev. B **79**, 100506 (2009).
[17] P. J. Hirschfeld and N. Goldenfeld, Phys. Rev. B **48**, 4219 (1993).
[18] X. G. Luo, M. A. Tanatar, J.-P. Reid, H. Shakeripour, N. Doiron-Leyraud, N. Ni, S. L. Bud'ko, P. C. Canfield, H. Luo, Z. Wang, H.-H. Wen, R. Prozorov, and L. Taillefer, Phys. Rev. B **80**, 140503 (2009).
[19] A. B. Vorontsov, M. G. Vavilov, and A. V. Chubukov, Phys. Rev. B **79**, 140507 (2009).
[20] Y. Bang, EPL **86**, 47001 (2009).
[21] V. G. Kogan, Phys. Rev. B **81**, 184528 (2010).
[22] R. T. Gordon, H. Kim, M. A. Tanatar, R. Prozorov, and V. G. Kogan, Phys. Rev. B **81**, 180501 (2010).
[23] A. I. Coldea, J. D. Fletcher, A. Carrington, J. G. Analytis, A. F. Bangura, J.-H. Chu, A. S. Erickson, I. R. Fisher, N. E. Hussey, and R. D. McDonald, Phys. Rev. Lett. **101**, 216402 (2008).
[24] J. D. Fletcher, A. Serafin, L. Malone, J. G. Analytis, J.-H. Chu, A. S. Erickson, I. R. Fisher, and A. Carrington, Phys. Rev. Lett. **102**, 147001 (2009).
[25] K. Hashimoto, M. Yamashita, S. Kasahara, Y. Senshu, N. Nakata, S. Tonegawa, K. Ikada, A. Serafin, A. Carrington, T. Terashima, H. Ikeda, T. Shibauchi, and Y. Matsuda, Phys. Rev. B **81**, 220501(R) (2010).
[26] M. Yamashita, N. Nakata, Y. Senshu, S. Tonegawa, K. Ikada, K. Hashimoto, H. Sugawara, T. Shibauchi, and Y. Matsuda, Phys. Rev. B **80**, 220509 (2009).
[27] A. Ganin, D. V. Giap, J. Claridge, J. Bacsa, J. Gould, and M. Rosseinsky (unpublished).

[28] A. Carrington, R. W. Giannetta, J. T. Kim, and J. Giapintzakis, Phys. Rev. B **59**, R14173 (1999).
[29] J. D. Fletcher, A. Carrington, P. Diener, P. Rodiere, J. P. Brison, R. Prozorov, T. Olheiser, and R. W. Giannetta, Phys. Rev. Lett. **98**, 057003 (2007).
[30] R. Prozorov, R. W. Giannetta, A. Carrington, and F. M. Araujo-Moreira, Phys. Rev. B **62**, 115 (2000).
[31] Omega Engineering Inc., One Omega Drive, Stamford, Connecticut, USA.
[32] P. F. Sullivan and G. Seidel, Phys. Rev. **173**, 679 (1968).
[33] B. L. Brandt, D. W. Liu, and L. G. Rubin, Rev. Sci. Instrum. **70**, 104 (1999).
[34] Type-E thermocouple reference table from NIST Monograph 175.
[35] Self-sensentive microcantilever. SII NanoTechnology Inc., Chuo-ku Tokyo, Japan. Model number: SSI-SS-ML-PRC120.
[36] K. Hashimoto, A. Serafin, S. Tonegawa, R. Katsumata, R. Okazaki, T. Saito, H. Fukazawa, Y. Kohori, K. Kihou, C. H. Lee, A. Iyo, H. Eisaki, H. Ikeda, Y. Matsuda, A. Carrington, and T. Shibauchi, Phys. Rev. B **82**, 014526 (2010).
[37] J. R. Cooper, Phys. Rev. B **54**, R3753 (1996).
[38] P. K. Biswas, G. Balakrishnan, D. M. Paul, C. V. Tomy, M. R. Lees, and A. D. Hillier, Phys. Rev. B **81**, 092510 (2010).
[39] J. K. Dong, T. Y. Guan, S. Y. Zhou, X. Qiu, L. Ding, C. Zhang, U. Patel, Z. L. Xiao, and S. Y. Li, Phys. Rev. B **80**, 024518 (2009).
[40] M. Bendele, S. Weyeneth, R. Puzniak, A. Maisuradze, E. Pomjakushina, K. Conder, V. Pomjakushin, H. Luetkens, S. Katrych, A. Wisniewski, R. Khasanov, and H. Keller, Phys. Rev. B **81**, 224520 (2010).
[41] J. E. Sonier, J. H. Brewer, R. F. Kiefl, G. D. Morris, R. I. Miller, D. A. Bonn, J. Chakhalian, R. H. Heffner, W. N. Hardy, and R. Liang, Phys. Rev. Lett. **83**, 4156 (1999).
[42] H. Kim, C. Martin, R. T. Gordon, M. A. Tanatar, J. Hu, B. Qian, Z. Q. Mao, R. Hu, C. Petrovic, N. Salovich, R. Giannetta, and R. Prozorov, Phys. Rev. B **81**, 180503 (2010).
[43] H. Padamsee, J. Neighbor, and C. Shiffman, J. Low Temp. Phys. **12**, 387 (1973).
[44] O. J. Taylor, A. Carrington, and J. A. Schlueter, Phys. Rev. Lett. **99**, 057001 (2007).
[45] S. E. Inderhees, M. B. Salamon, J. P. Rice, and D. M. Ginsberg, Phys. Rev. Lett. **66**, 232 (1991).
[46] N. Overend, M. A. Howson, and I. D. Lawrie, Phys. Rev. Lett. **72**, 3238 (1994).
[47] A. Junod, K. Q. Wang, T. Tsukamoto, G. Triscone, B. Revaz, E. Walker, and J. Muller, Physica C **229**, 209 (1994).
[48] A. Carrington, C. Marcenat, F. Bouquet, D. Colson, A. Bertinotti, J. F. Marucco, and J. Hammann, Phys. Rev. B **55**, R8674 (1997).
[49] A. Schilling, R. A. Fisher, N. E. Phillips, U. Welp, W. K. Kwok, and G. W. Crabtree, Phys. Rev. Lett. **78**, 4833 (1997).
[50] J. A. Lipa and T. C. P. Chui, Phys. Rev. Lett. **51**, 2291 (1983).
[51] D. S. Fisher, M. P. A. Fisher, and D. A. Huse, Phys. Rev. B **43**, 130 (1991).
[52] N. Doiron-Leyraud, C. Proust, D. Leboeuf, J. Levallois, J. B. Bonnemaison, R. X. Liang, D. A. Bonn, W. N. Hardy, and L. Taillefer, Nature (London) **447**, 565 (2007).
[53] A. F. Bangura, J. D. Fletcher, A. Carrington, J. Levallois, M. Nardone, B. Vignolle, P. J. Heard, N. Doiron-Leyraud, D. LeBoeuf, L. Taillefer, S. Adachi, C. Proust, and N. E. Hussey, Phys. Rev. Lett. **100**, 047004 (2008).
[54] Z. Pribulova, T. Klein, J. Kacmarcik, C. Marcenat, M. Konczykowski, S. L. Bud'ko, M. Tillman, and P. C. Canfield, Phys. Rev. B **79**, 020508 (2009).
[55] A. Carrington, A. P. Mackenzie, and A. Tyler, Phys. Rev. B **54**, R3788 (1996).
[56] V. B. Geshkenbein, L. B. Ioffe, and A. J. Millis, Phys. Rev. Lett. **80**, 5778 (1998).
[57] D. Braithwaite, G. Lapertot, W. Knafo, and I. Sheikin, J. Phys. Soc. Jpn. **79**, 053703 (2010).
[58] S. Khim, J. W. Kim, E. S. Choi, Y. Bang, M. Nohara, H. Takagi, and K. H. Kim, Phys. Rev. B **81**, 184511 (2010).
[59] V. Tsurkan, J. Deisenhofer, A. Günther, C. Kant, H.-A. K. von Nidda, F. Schrettle, and A. Loidl, arXiv:1006.4453 (unpublished).